Kinematics in Iterated Correlations of a Passive Acoustic Experiment

Sjoerd de Ridder and George Papanicolaou

ABSTRACT

Correlating ambient seismic noise can yield the inter-station Green's function, but only if the energy that is excited by seismic background sources is sufficiently equipartitioned after averaging over all sources. If this requirement is not fulfilled, the reconstructed Green's function is imperfect. Secondary scattering can mitigate the directivity of the primary wave field emitted by the sources. To extract and utilize secondary scattering for Green's function reconstruction, we introduce a second correlation using an auxiliary station. We investigate the kinematics of the reconstructed Green's functions to understand the role of the positions of source, scatterer and auxiliary stations. Iterated correlations can use secondary scattering to mitigate the directivity in the background seismic wave field. In general, there will be additional spurious events in the retrieved Green's functions. Averaging the results of several sources and using a network of randomly distributed auxiliary stations can minimize these spurious events with respect to the correct events in the retrieved Green's functions.

INTRODUCTION

It has long been known that correlations of seismic background noise recorded at two stations can yield the Green's function between the two stations (Aki, 1957; Claerbout, 1968; Lobkis and Weaver, 2001; Wapenaar, 2004), hereafter referred to as the estimated Green's function (EGF). A variety of proofs exist for this relation, including many based upon diffusivity of the wave fields (Weaver and Lobkis, 2001; Roux et al., 2005; Sánchez-Sesma et al., 2006; Sánchez-Sesma and Campillo, 2006), stationary-phase analysis (Schuster et al., 2004; Snieder, 2004; Snieder et al., 2006), and propagation invariants and reciprocity theorems (Claerbout, 1976; Weaver and Lobkis, 2004; Wapenaar, 2004; Wapenaar and Fokkema, 2006; van Manen et al., 2005). In general, these proofs require energy equipartitioning in the background seismic field; i.e., the energy flow must be equal in all directions. It is generally assumed that energy equipartitioning should be obtained after averaging over sources that excite the background field (Snieder et al., 2007). If the background noise field does not satisfy this condition, we expect the field correlations to recover imperfect EGFs (Malcolm et al., 2004; Paul et al., 2005).

Recently it has been argued that multiple scattering by random inhomogeneities

can excite a secondary wave field that satisfies the assumption of equipartitioning, even if the primary wave field does not (Stehly et al., 2008). It is also known that correlation of coda waves can yield the Green's function (Snieder, 2004; Malcolm et al., 2004; Paul et al., 2005; de Ridder, 2008). Stehly et al. (2008) describes a way to use the coda waves of background noise to improve the quality of EGFs (Stehly et al., 2008). Garnier and Papanicolaou (2009) give a proof for this procedure to enhance Green's function estimation in random media based upon stationary-phase analysis of the four leading terms in the higher order correlation.

This paper discusses the problems associated with Green's function retrieval in directional wave fields. Then we proceed to briefly repeat the stationary-phase analysis of Garnier and Papanicolaou (2009) in the case of a wave field excited by one source in a homogeneous medium with the addition of one scatterer. The kinematics of the four leading terms are investigated using correlation gathers of auxiliary station position and source positions. Our examples show the basic procedure for reconstructing a Green's function by iterated correlations and provides a physical understanding of the elementary requirements for the positions of sources, random inhomogeneities, and auxiliary stations. This study has implications for seismic exploration using ambient seismic noise for different acquisition geometries, as in a network of stations only on the surface recording the ambient field above a reservoir, or a borehole survey with stations both down-hole and on the surface.

CONVENTIONAL VERSUS ITERATIVE INTERFEROMETRY

Conventional seismic interferometry (SI) retrieves the Green's function between two stations by correlating, $C^{(2)}$, records of an ambient field, in which the energy is equipartitioned, recorded at both stations. It is generally assumed that energy equipartitioning should be obtained after averaging over sources that excite the background field (Snieder et al., 2007). Sources located at stationary phases are necessary to retrieve high-quality EGFs. For example, the stationary-phase region of the Green's function between stations A and B in Figure 1(a) is located on a ray path from station B extending to and beyond station A [gray shading on left side of Figure 1(a)]. Correlating responses from these sources recorded at A and B will retrieve a high-quality EGF. However, because the sources in Figure 5(b) are not located in the stationary-phase region, correlating responses from these sources recorded at A and B will retrieve a low-quality EGF.

Some proposed methods to compensate for anisotropic illuminations include: (a) Beam forming and weighting (Stork and Cole, 2007) or $\tau - p$ filtering (Ruigrok et al., 2008) the data for different directionality components. (b) Estimating a radiation pattern by autocorrelating the down-going wave field and correcting by deconvolution (van der Neut et al., 2008; van der Neut and Bakulin, 2008). (c) Multidimensional deconvolution after the identification of individual responses (Wapenaar et al., 2008). Finally (d), Stehly et al. (2008) propose a novel procedure to improve EGFs by using

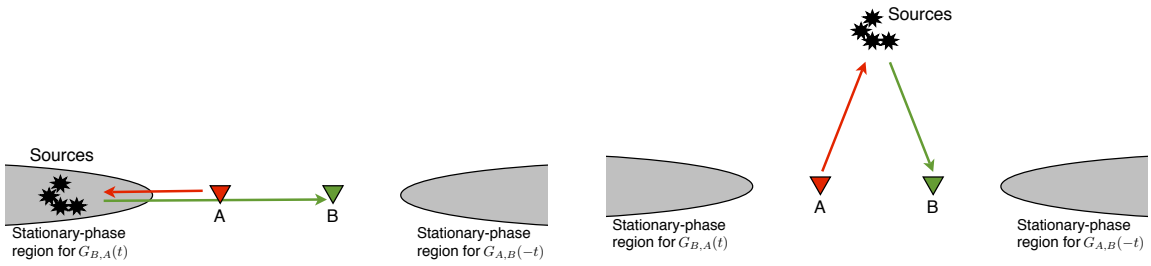

(a) (b)

Figure 1: Source positions for respectively (a) high-quality and (b) poor quality Green's function estimation by conventional SI. Stationary-phase regions are indicated by gray areas. [**NR**]

scatterers positioned at the stationary-phase positions that act as secondary Huygens' sources, as illustrated in Figure 2. Their method requires three steps: First, the recordings at two main stations are correlated with a network of auxiliary stations. Each correlation yields an EGF. Second, each EGF is muted for times prior to an estimated arrival time. Third, a correlation, C^3, is evaluated between the muted EGF pairs estimated for each auxiliary station. That correlation is subsequently averaged across the network of auxiliary stations.

Figure 2: Illustration of how scatterers acting as secondary Huygens' sources can illuminate stations A and B from a stationary-phase region, while the primary sources are located outside the stationary-phase regions. [**NR**]

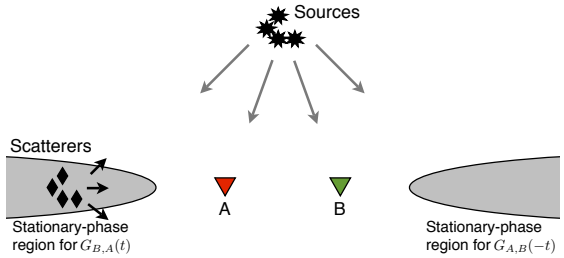

GREEN'S FUNCTION RETRIEVAL BY CORRELATION

We define the temporal correlation function between two time signals $F_A(t)$ and $F_B(t)$ measured at stations A and B as

$$C^{(2)}_{B,A}(t) = \int_{-\infty}^{\infty} F_B(\tau + t) F_A(\tau) \mathrm{d}\tau = \frac{1}{2\pi} \int_{-\infty}^{\infty} F_B(\omega) F^*_A(\omega) \, \exp\{i\omega t\} \, \mathrm{d}\omega, \qquad (1)$$

where ω denotes angular frequency. The right-hand side of equation 1 shows that through the inverse Fourier transformation of equation A-3, a correlation integral in the time domain is a direct product in the frequency domain. We can retrieve the Green's function between two stations A and B by independently measuring responses

of sources positioned on a boundary surrounding the two stations, and summing the correlation between the measurements at the two stations. This property can be expressed as[1] (Wapenaar and Fokkema, 2006):

$$G(\mathbf{x}_B, \mathbf{x}_A, \omega) - G^*(\mathbf{x}_A, \mathbf{x}_B, \omega) = -\frac{2i\omega}{c_0} \oint_{\partial \mathbf{D}} G(\mathbf{x}_B, \mathbf{x}_s, \omega) G^*(\mathbf{x}_A, \mathbf{x}_s, \omega) \mathrm{d}\mathbf{x}_s, \quad (2)$$

where $\mathbf{x}_A$, $\mathbf{x}_B$ and $\mathbf{x}_s$ denote positions of stations A and B and the sources respectively.

We investigate the terms within this this integral for a medium containing a scatterer. The Green's function under the Born approximation in a scattering medium is composed of two terms:

$$G(\mathbf{x}, \mathbf{x}_s, \omega) = G_0(\mathbf{x}, \mathbf{x}_s, \omega) + G_1(\mathbf{x}, \mathbf{x}_s, \omega), \quad (3)$$

where G_0 is the contribution of the direct wave, and G_1 is the contribution of the scattered wave. In the Born approximation, the contribution of the scatterer is included to order α. The correlation product between measurements made at stations A and B therefore is composed of $2^2 = 4$ terms

$$\begin{aligned} C^{(2)}_{B,A}(\omega) = {} & G_0(\mathbf{x}_B, \mathbf{x}_s, \omega) G_0^*(\mathbf{x}_A, \mathbf{x}_s, \omega) + G_0(\mathbf{x}_B, \mathbf{x}_s, \omega) G_1^*(\mathbf{x}_A, \mathbf{x}_s, \omega) + \\ & G_1(\mathbf{x}_B, \mathbf{x}_s, \omega) G_0^*(\mathbf{x}_A, \mathbf{x}_s, \omega) + G_1(\mathbf{x}_B, \mathbf{x}_s, \omega) G_1^*(\mathbf{x}_A, \mathbf{x}_s, \omega), \end{aligned} \quad (4)$$

which will be referred to as 4.1, 4.2, 4.3 and 4.4 respectively. The second and third terms are of order α, and the fourth term is of order α^2. Therefore, we should exclude the fourth term when we evaluate the right-hand side of equation 2 and compare it to the left-hand side of equation 2. See Snieder et al. (2008) for a more general discussion

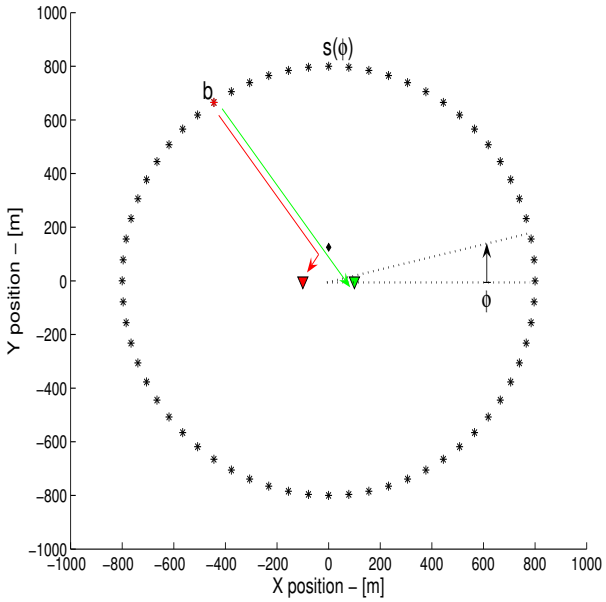

Figure 3: Geometry for the evaluation of $C^{(2)}_{B,A}$ in a homogeneous medium containing one scatterer. For three source positions, a, b and c, two ray paths are shown for stationary phases; see text. [**ER**]

[1] We employ a different definition of the Green's function with respect to equation 31 of Wapenaar and Fokkema (2006), $G' = \frac{\rho}{i\omega} G$, where ρ is density.

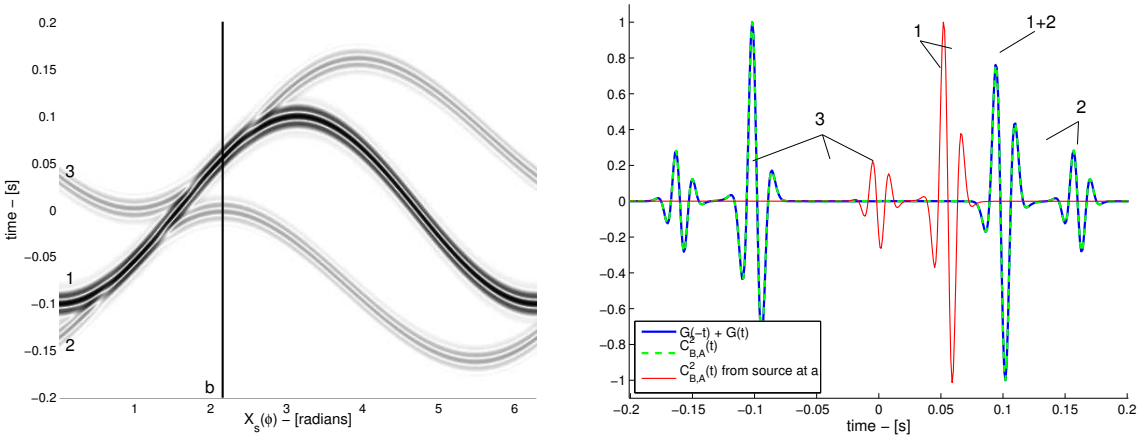

(a) (b)

Figure 4: a) Correlogram displaying correlations of source responses measured at stations A and B for sources as a function of position angle. b) Comparison of retrieved and true Green's functions. [**ER**]

of the fourth term for exact Green's functions (without Born approximation). We denote the integration of $C^{(2)}_{B,A}$ over the source coordinate and multiplication by the phase-modifying factor as follows:

$$\tilde{C}^{(2)}_{B,A}(\omega) = -\frac{2i\omega}{c_0} \oint_{\partial \mathbf{D}} C^{(2)}_{B,A}(\omega) \mathrm{d}\mathbf{x}_s, \tag{5}$$

where $C^{(2)}_{B,A}(\omega)$ is an implicit function of source position $\mathbf{x}_s$, according to equation 4.

STATIONARY-PHASE ANALYSIS OF CONVENTIONAL INTERFEROMETRY

The phase of the correlation under the integral on the right-hand side of equation 2 changes rapidly as a function of source position. The dominant contribution to the integral comes from points at which the phase is stationary. Physically these positions correspond to source points from where the ray paths to both stations align. To analyze the stationary phases in the presence of a scatterer, we consider a homogeneous medium and study the time-domain expression of equation 2 using the

first three terms in $C^{(2)}_{B,A}$ of equation 4:

$$\begin{aligned} G(\mathbf{x}_B,\mathbf{x}_A,t) - G(\mathbf{x}_A,\mathbf{x}_B,-t) = & \qquad (6)\\ \tilde{C}^{(2)}_{B,A}(t) = -\int_{-\infty}^{\infty} \frac{2i\omega}{2\pi c_0} \oint_{\partial\mathbf{D}} & a_0(\mathbf{x}_B,\mathbf{x}_s,\omega)a_0^*(\mathbf{x}_A,\mathbf{x}_s,\omega)\exp\{i\Omega_1\} \quad + \\ & a_0(\mathbf{x}_B,\mathbf{x}_s,\omega)a_1^*(\mathbf{x}_A,\mathbf{x}_s,\omega)\exp\{i\Omega_2\} \quad + \\ & a_1(\mathbf{x}_B,\mathbf{x}_s,\omega)a_0^*(\mathbf{x}_A,\mathbf{x}_s,\omega)\exp\{i\Omega_3\} \quad \mathrm{d}\mathbf{x}_s\mathrm{d}\omega, \end{aligned}$$

where a_0 and a_1 are amplitude factors. The rapid phases, $\Omega_1 = \Omega_1(\mathbf{x}_s,\mathbf{x}_A,\mathbf{x}_B,\omega)$, $\Omega_2(\mathbf{x}_s,\mathbf{x}_A,\mathbf{x}_B,\omega)$ and $\Omega_3(\mathbf{x}_s,\mathbf{x}_A,\mathbf{x}_B,\omega)$, of the three terms are found using equations A-6 and A-11:

$$\Omega_1 = \omega\left[t - c_0^{-1}\left\{|\mathbf{x}_B-\mathbf{x}_s| - |\mathbf{x}_A-\mathbf{x}_s|\right\}\right], \qquad (7)$$

$$\Omega_2 = \omega\left[t - c_0^{-1}\left\{|\mathbf{x}_B-\mathbf{x}_s| - |\mathbf{x}_A-\mathbf{x}_c| - |\mathbf{x}_c-\mathbf{x}_s|\right\}\right], \qquad (8)$$

$$\Omega_3 = \omega\left[t - c_0^{-1}\left\{|\mathbf{x}_B-\mathbf{x}_c| + |\mathbf{x}_c-\mathbf{x}_s| - |\mathbf{x}_A-\mathbf{x}_s|\right\}\right], \qquad (9)$$

where $\mathbf{x}_c$ is the position of the scatterer.

We analyze these rapid phases using the stationary-phase method, keeping $\mathbf{x}_A$ and $\mathbf{x}_B$ fixed and varying $\mathbf{x}_s$. According to the stationary-phase method, the dominant contribution comes from stationary phases where

$$\partial_\omega\Omega = 0 \quad \text{and} \quad \nabla_{\mathbf{x}_s}\Omega = \mathbf{0}. \qquad (10)$$

From the rapid phase, Ω_1, of the first term in equation 6, we find stationary points for which

$$t = c_0^{-1}\left\{|\mathbf{x}_B-\mathbf{x}_s| - |\mathbf{x}_A-\mathbf{x}_s|\right\} \quad \text{and} \quad \nabla_{\mathbf{x}_s}|\mathbf{x}_B-\mathbf{x}_s| = \nabla_{\mathbf{x}_s}|\mathbf{x}_A-\mathbf{x}_s|. \qquad (11)$$

The second condition requires the points $\mathbf{x}_A$ and $\mathbf{x}_B$ to be aligned along a line issuing from $\mathbf{x_s}$. When the stations and source are aligned as $\mathbf{x}_s \rightarrow \mathbf{x}_A \rightarrow \mathbf{x}_B$, the first condition gives $t = c_0^{-1}\left\{|\mathbf{x}_B-\mathbf{x}_A|\right\}$. When the stations and source are aligned as $\mathbf{x}_s \rightarrow \mathbf{x}_B \rightarrow \mathbf{x}_A$, the first condition gives $t = -c_0^{-1}\left\{|\mathbf{x}_B-\mathbf{x}_A|\right\}$.

From rapid phase Ω_2 of the second terms in equation 6, we find stationary points for which

$$t = c_0^{-1}\left\{|\mathbf{x}_B-\mathbf{x}_s| - |\mathbf{x}_A-\mathbf{x}_c| - |\mathbf{x}_c-\mathbf{x}_s|\right\} \text{ and } \nabla_{\mathbf{x}_s}|\mathbf{x}_B-\mathbf{x}_s| = \nabla_{\mathbf{x}_s}|\mathbf{x}_c-\mathbf{x}_s|. \qquad (12)$$

The second condition requires the points $\mathbf{x}_B$ and $\mathbf{x}_c$ to be on a line issuing from $\mathbf{x}_s$. When station B, as well as the scatterer and sources are aligned as $\mathbf{x}_s \rightarrow \mathbf{x}_B \rightarrow \mathbf{x}_c$, then $|\mathbf{x}_c-\mathbf{x}_s| = |\mathbf{x}_c-\mathbf{x}_B| + |\mathbf{x}_B-\mathbf{x}_s|$, and the first condition states that $t = -c_0^{-1}\left\{|\mathbf{x}_B-\mathbf{x}_c| + |\mathbf{x}_c-\mathbf{x}_A|\right\}$. When station B, the scatterer and the source are aligned as $\mathbf{x}_s \rightarrow \mathbf{x}_c \rightarrow \mathbf{x}_B$, then $|\mathbf{x}_B-\mathbf{x}_s| = |\mathbf{x}_c-\mathbf{x}_s| + |\mathbf{x}_B-\mathbf{x}_c|$, and the first condition states that $t = c_0^{-1}\left\{|\mathbf{x}_B-\mathbf{x}_c| - |\mathbf{x}_A-\mathbf{x}_c|\right\}$.

From rapid phase Ω_3 of the second terms in equation 6, we find stationary points for which

$$t = c_0^{-1}\left\{|\mathbf{x}_B - \mathbf{x}_c| + |\mathbf{x}_c - \mathbf{x}_s| - |\mathbf{x}_A - \mathbf{x}_s|\right\} \quad \text{and} \quad \nabla_{\mathbf{x}_s}|\mathbf{x}_A - \mathbf{x}_s| = \nabla_{\mathbf{x}_s}|\mathbf{x}_c - \mathbf{x}_s|. \tag{13}$$

The second condition requires the points $\mathbf{x}_A$ and $\mathbf{x}_c$ to be on a line issuing from $\mathbf{x}_s$. When station A, as well as the scatterer and sources are aligned as $\mathbf{x}_s \rightarrow \mathbf{x}_A \rightarrow \mathbf{x}_c$, then $|\mathbf{x}_c - \mathbf{x}_s| = |\mathbf{x}_c - \mathbf{x}_A| + |\mathbf{x}_A - \mathbf{x}_s|$, and the first condition states that $t = c_0^{-1}\left\{|\mathbf{x}_B - \mathbf{x}_c| + |\mathbf{x}_c - \mathbf{x}_A|\right\}$. When station A, the scatterer and sources are aligned as $\mathbf{x}_s \rightarrow \mathbf{x}_c \rightarrow \mathbf{x}_A$, then $|\mathbf{x}_A - \mathbf{x}_s| = |\mathbf{x}_A - \mathbf{x}_c| + |\mathbf{x}_c - \mathbf{x}_s|$, and the first condition states that $t = c_0^{-1}\left\{|\mathbf{x}_B - \mathbf{x}_c| - |\mathbf{x}_A - \mathbf{x}_c|\right\}$. For a more extensive treatment of stationary-phase positions in conventional interferometry, see Schuster et al. (2004); Snieder (2004); Snieder et al. (2006) and Garnier and Papanicolaou (2009).

EXAMPLE OF GREEN'S FUNCTION RETRIEVAL BY CONVENTIONAL INTERFEROMETRY

To aid interpretation of iterated interferometry in later sections, we study the kinematics of conventional interferometry for a medium containing a scatterer. The background velocity is $c_0 = 2000$ m/s. Stations A and B are positioned 200 m distant from each other, and the scatterer is positioned 125 m above and in between the stations. The stations and scatterer are surrounded by 512 sources on a circle with a radius of 800 m, centered between the two stations; see Figure 3.

We simulate the measurements at stations A and B using the single-scatterer Born approximation (see appendix equation A-11). We assume all sources emit a zero-phase Ricker wavelet, $s(t)$ (see appendix equation A-8). For each source location separately, the responses recorded at stations A and B are cross-correlated, and their contribution to the integral on the right-hand side of equation 2 is shown as a function of angle in the correlogram in Figure 4(a).

The correlogram contains three events labeled 1, 2 and 3. These correspond to the first three terms respectively in the correlation product in equation 4. Term 1 is associated with the direct event between stations A and B. It has two stationary points at angles of $\phi = 0$ and $\phi = \pi$ radians, where the stations and source are aligned on a line as $\mathbf{x}_s \rightarrow \mathbf{x}_B \rightarrow \mathbf{x}_A$ and $\mathbf{x}_s \rightarrow \mathbf{x}_A \rightarrow \mathbf{x}_B$, respectively. For all other angles, the correlation peak resides at a lag that is smaller than the actual travel time between the stations. The second and third terms correspond to correlations of recorded events that are either scattered at A and direct at B or vice versa. Both events have two stationary phases. Event 2, for example, has a stationary phase for a source positioned close to $\phi = 3/4\pi$ where $\mathbf{x}_s \rightarrow \mathbf{x}_c \rightarrow \mathbf{x}_B$, and at approximately $\phi = 4/3\pi$ where $\mathbf{x}_s \rightarrow \mathbf{x}_B \rightarrow \mathbf{x}_c$. The total correlogram is summed over all angles and multiplied by a factor $-\frac{2i\omega}{c_0}$, according to equation 5, to match the asymmetrized true Green's function on the left-hand side of equation 2. The asymmetrized Green's function is multiplied with the auto-correlation of the Ricker wavelet to match the source function after

correlations. Although the calculation matches before normalization, the Green's functions are normalized to have a peak value of 1. The comparison between the retrieved result (dashed green line) found by evaluating the right-hand side of equation 2 and the directly modeled result (solid blue curve) found by computing the left-hand side of equation 2 is shown in Figure 4(b), they match exactly.

Three contributions of stationary angles are isolated from all other source contributions and compared to the fully retrieved result. These stationary angles have events arriving with the correct travel time but incorrect phase. They also have events with incorrect travel times. However the contribution from a source positioned close to $\phi = 4/3\pi$ radians seems to have an event with a travel time approximately corresponding to the acausal direct event. It is non-stationary and associated with the acausal scattered events as can be seen in Figure 4(a).

GREEN'S FUNCTION RETRIEVAL BY ITERATED CORRELATIONS

In the absence of complete source coverage, we can make use of the scattering properties of the medium to mitigate the directivity of the wave field. The iterated correlation between stations B and A is defined using auxiliary station X as follows:

$$\begin{aligned} C^{(3)}_{B,A}(t) &= \int_{-\infty}^{\infty} C^{(2)}_{B,X}(\tau' + t) C^{(2)}_{A,X}(\tau') \mathrm{d}\tau' \\ &= \int_{-\infty}^{\infty}\int_{-\infty}^{\infty}\int_{-\infty}^{\infty} F_B(\tau + \tau' + t) F_X(\tau) F_X(s) F_A(s + \tau') \mathrm{d}s \mathrm{d}\tau \mathrm{d}\tau' \\ &= \frac{1}{2\pi}\int_{-\infty}^{\infty} F_B(\omega) F^*_X(\omega) F_X(\omega) F^*_A(\omega)\, \exp\{i\omega t\}\, \mathrm{d}\omega \end{aligned} \tag{14}$$

The Green's function in the Born approximation for a scattering medium is com-

posed of two terms; $C^{(3)}_{B,A}$ therefore contains $2^4 = 16$ terms

$$
\begin{aligned}
C^{(3)}_{B,A} = {} & G_0(\mathbf{x}_B,\mathbf{x}_s,\omega)G_0^*(\mathbf{x}_X,\mathbf{x}_s,\omega)G_0^*(\mathbf{x}_A,\mathbf{x}_s,\omega)G_0(\mathbf{x}_X,\mathbf{x}_s,\omega) + && (15.1)\\
& G_0(\mathbf{x}_B,\mathbf{x}_s,\omega)G_0^*(\mathbf{x}_X,\mathbf{x}_s,\omega)G_0^*(\mathbf{x}_A,\mathbf{x}_s,\omega)G_1(\mathbf{x}_X,\mathbf{x}_s,\omega) + && (15.2)\\
& G_0(\mathbf{x}_B,\mathbf{x}_s,\omega)G_0^*(\mathbf{x}_X,\mathbf{x}_s,\omega)G_1^*(\mathbf{x}_A,\mathbf{x}_s,\omega)G_0(\mathbf{x}_X,\mathbf{x}_s,\omega) + && (15.3)\\
& G_0(\mathbf{x}_B,\mathbf{x}_s,\omega)G_0^*(\mathbf{x}_X,\mathbf{x}_s,\omega)G_1^*(\mathbf{x}_A,\mathbf{x}_s,\omega)G_1(\mathbf{x}_X,\mathbf{x}_s,\omega) + && (15.4)\\
& G_0(\mathbf{x}_B,\mathbf{x}_s,\omega)G_1^*(\mathbf{x}_X,\mathbf{x}_s,\omega)G_0^*(\mathbf{x}_A,\mathbf{x}_s,\omega)G_0(\mathbf{x}_X,\mathbf{x}_s,\omega) + && (15.5)\\
& G_0(\mathbf{x}_B,\mathbf{x}_s,\omega)G_1^*(\mathbf{x}_X,\mathbf{x}_s,\omega)G_0^*(\mathbf{x}_A,\mathbf{x}_s,\omega)G_1(\mathbf{x}_X,\mathbf{x}_s,\omega) + && (15.6)\\
& G_0(\mathbf{x}_B,\mathbf{x}_s,\omega)G_1^*(\mathbf{x}_X,\mathbf{x}_s,\omega)G_1^*(\mathbf{x}_A,\mathbf{x}_s,\omega)G_0(\mathbf{x}_X,\mathbf{x}_s,\omega) + && (15.7)\\
& G_0(\mathbf{x}_B,\mathbf{x}_s,\omega)G_1^*(\mathbf{x}_X,\mathbf{x}_s,\omega)G_1^*(\mathbf{x}_A,\mathbf{x}_s,\omega)G_1(\mathbf{x}_X,\mathbf{x}_s,\omega) + && (15.8)\\
& G_1(\mathbf{x}_B,\mathbf{x}_s,\omega)G_0^*(\mathbf{x}_X,\mathbf{x}_s,\omega)G_0^*(\mathbf{x}_A,\mathbf{x}_s,\omega)G_0(\mathbf{x}_X,\mathbf{x}_s,\omega) + && (15.9)\\
& G_1(\mathbf{x}_B,\mathbf{x}_s,\omega)G_0^*(\mathbf{x}_X,\mathbf{x}_s,\omega)G_0^*(\mathbf{x}_A,\mathbf{x}_s,\omega)G_1(\mathbf{x}_X,\mathbf{x}_s,\omega) + && (15.10)\\
& G_1(\mathbf{x}_B,\mathbf{x}_s,\omega)G_0^*(\mathbf{x}_X,\mathbf{x}_s,\omega)G_1^*(\mathbf{x}_A,\mathbf{x}_s,\omega)G_0(\mathbf{x}_X,\mathbf{x}_s,\omega) + && (15.11)\\
& G_1(\mathbf{x}_B,\mathbf{x}_s,\omega)G_0^*(\mathbf{x}_X,\mathbf{x}_s,\omega)G_1^*(\mathbf{x}_A,\mathbf{x}_s,\omega)G_1(\mathbf{x}_X,\mathbf{x}_s,\omega) + && (15.12)\\
& G_1(\mathbf{x}_B,\mathbf{x}_s,\omega)G_1^*(\mathbf{x}_X,\mathbf{x}_s,\omega)G_0^*(\mathbf{x}_A,\mathbf{x}_s,\omega)G_0(\mathbf{x}_X,\mathbf{x}_s,\omega) + && (15.13)\\
& G_1(\mathbf{x}_B,\mathbf{x}_s,\omega)G_1^*(\mathbf{x}_X,\mathbf{x}_s,\omega)G_0^*(\mathbf{x}_A,\mathbf{x}_s,\omega)G_1(\mathbf{x}_X,\mathbf{x}_s,\omega) + && (15.14)\\
& G_1(\mathbf{x}_B,\mathbf{x}_s,\omega)G_1^*(\mathbf{x}_X,\mathbf{x}_s,\omega)G_1^*(\mathbf{x}_A,\mathbf{x}_s,\omega)G_0(\mathbf{x}_X,\mathbf{x}_s,\omega) + && (15.15)\\
& G_1(\mathbf{x}_B,\mathbf{x}_s,\omega)G_1^*(\mathbf{x}_X,\mathbf{x}_s,\omega)G_1^*(\mathbf{x}_A,\mathbf{x}_s,\omega)G_1(\mathbf{x}_X,\mathbf{x}_s,\omega). && (15.16)
\end{aligned}
\qquad (15)
$$

Three groups of terms can be distinguished; group 1 includes terms 15.1, 15.2, 15.3, 15.4, 15.5, 15.9 and 15.13, which are terms correlating with the dominant contribution in $C^{(2)}$; $G_0G_0^*$. Group 2 contains the terms of interest in this paper; 15.6, 15.7, 15.10 and 15.11; see the stationary-phase analysis below. The third group contains events that are of order α^3 and includes terms 15.8, 15.12, 15.14, 15.15 and 15.16. The leading term in $C^{(2)}$ contributes to a spurious term, because the source is not located at a stationary angle of the event between stations A and B. To exclude the terms of group 1, we remove the dominant term after forming $C^{(2)}_{B,X}$ and $C^{(2)}_{A,X}$. This is done by muting the correlation in the time domain to suppress all times smaller than τ_{coda}:

$$
\begin{aligned}
C^{(3)}_{B,A}(t) &= \int_{-\infty,-\tau'_{coda}}^{\tau'_{coda},\infty}\int_{-\infty}^{\infty}\int_{-\infty}^{\infty} F_B(\tau+\tau'+t)F_X(\tau)F_X(s)F_A(s+\tau')\mathrm{d}s\mathrm{d}\tau\mathrm{d}\tau' \quad (16)\\
&= \int_{-\infty}^{\infty}\int_{-\infty}^{\infty}\int_{-\infty}^{\infty} \beta(\tau')F_B(\tau+\tau'+t)F_X(\tau)F_X(s)F_A(s+\tau')\mathrm{d}s\mathrm{d}\tau\mathrm{d}\tau', \quad (17)
\end{aligned}
$$

where τ_{coda} is defined as an estimated traveltime between the main stations and the auxiliary stations, $\beta(\tau)$ is a muting function that is zero for $\beta(\tau) = 0$ for $\tau\ :\ [-\tau_{coda}:\tau_{coda}]$ and otherwise $\beta(\tau) = 1$.

We learned from Figure 3 that the dominant term always arrives within that time window. We average the iterated correlations over a network of A auxiliary stations and include a phase-modifying term,

$$
\tilde{C}^{(3)}_{B,A}(\omega) = \frac{2c_0}{i\omega A}\sum_{a=1}^{A} C^{(3)}_{B,A}(\omega), \qquad (18)
$$

where $\tilde{C}^{(3)}_{B,A}(\omega)$ is an implicit function of auxiliary-station position $\mathbf{x}_{X,a}$, according to equation 15. The phase-modifying proportionality factor is chosen such that the $\frac{\omega^2}{c_0^2}$ factor in the Born approximation (see equation A-10) is matched to the $\frac{-2i\omega}{c_0}$ factor in conventional interferometry (equation 2).

STATIONARY PHASES IN ITERATED CORRELATIONS

We proceed by studying the stationary phases of terms 15.6, 15.7, 15.10 and 15.11 in the iterated correlation. All terms correspond to particular combinations of ray paths.

Figure 5 shows for each term a graphical illustration of the combination of ray paths. Ray paths towards the source are subtracted from the ray paths emitting from the source, as in the correlation process (a convolution of one Green's function with the time reverse of another Green's function). The time domain of equation 15,

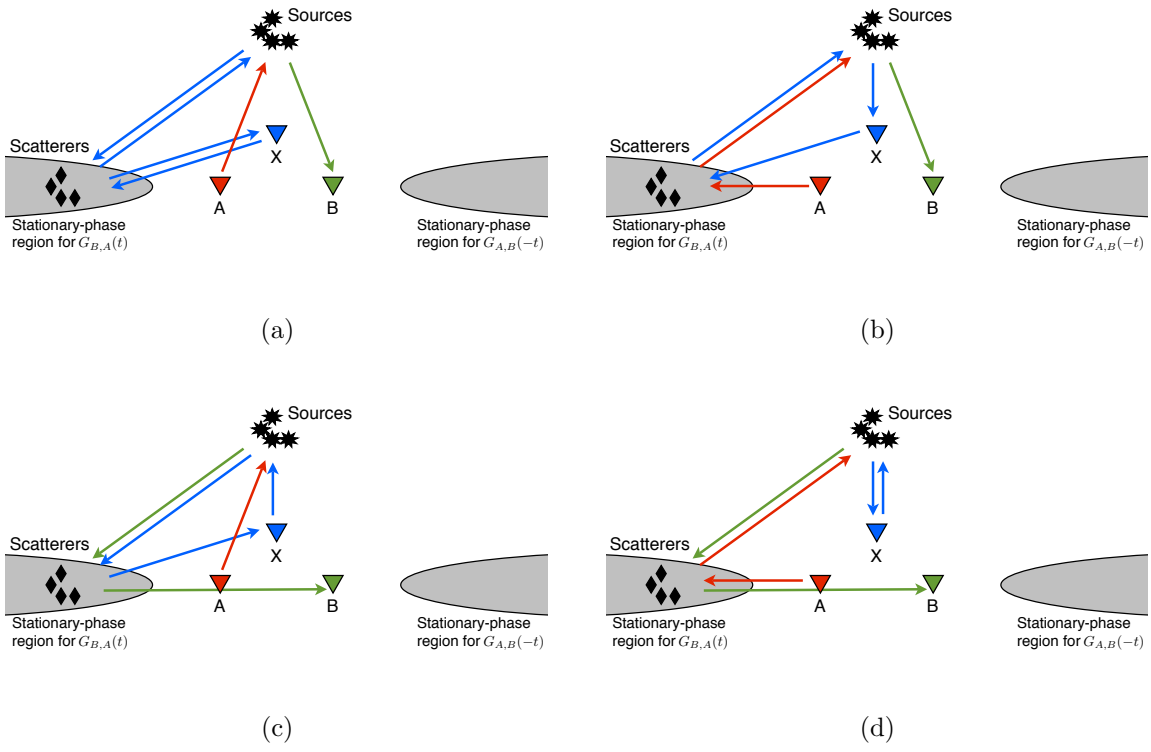

Figure 5: Geometrical interpretation of the correlations in terms 15.6, 15.7, 15.10 and 15.11 respectively in a) b) c) and d). [**NR**]

including only the terms of group 2, is given as

$$\begin{aligned}\tilde{C}^{(3)}_{B,A}(t) = \int_{-\infty}^{\infty} \frac{2c_0}{2\pi i\omega A} \sum_{a=1}^{A} \quad & (19)\\ a_0(\mathbf{x}_B,\mathbf{x}_s,\omega)a_1^*(\mathbf{x}_{X,a},\mathbf{x}_s,\omega)a_0^*(\mathbf{x}_A,\mathbf{x}_s,\omega)a_1(\mathbf{x}_{X,a},\mathbf{x}_s,\omega)\exp\{i\Omega_1\} \quad &+\\ a_0(\mathbf{x}_B,\mathbf{x}_s,\omega)a_1^*(\mathbf{x}_{X,a},\mathbf{x}_s,\omega)a_1^*(\mathbf{x}_A,\mathbf{x}_s,\omega)a_0(\mathbf{x}_{X,a},\mathbf{x}_s,\omega)\exp\{i\Omega_2\} \quad &+\\ a_1(\mathbf{x}_B,\mathbf{x}_s,\omega)a_0^*(\mathbf{x}_{X,a},\mathbf{x}_s,\omega)a_0^*(\mathbf{x}_A,\mathbf{x}_s,\omega)a_1(\mathbf{x}_{X,a},\mathbf{x}_s,\omega)\exp\{i\Omega_3\} \quad &+\\ a_1(\mathbf{x}_B,\mathbf{x}_s,\omega)a_0^*(\mathbf{x}_{X,a},\mathbf{x}_s,\omega)a_1^*(\mathbf{x}_A,\mathbf{x}_s,\omega)a_0(\mathbf{x}_{X,a},\mathbf{x}_s,\omega)\exp\{i\Omega_4\} \quad &\mathrm{d}\mathbf{x}_x\mathrm{d}\omega,\end{aligned}$$

where a_0 and a_1 are amplitude factors. The rapid phases, Ω_1, Ω_2, Ω_3 and Ω_4 are found using equations A-6 and A-11; for a particular auxiliary station $\mathbf{x}_X$, we find

$$\Omega_1 = \omega\left[t - c_0^{-1}\left\{|\mathbf{x}_B-\mathbf{x}_s| - |\mathbf{x}_A-\mathbf{x}_s|\right\}\right], \quad (20)$$

$$\Omega_2 = \omega\left[t - c_0^{-1}\left\{|\mathbf{x}_B-\mathbf{x}_s| - |\mathbf{x}_X-\mathbf{x}_c| - 2|\mathbf{x}_c-\mathbf{x}_s| - |\mathbf{x}_A-\mathbf{x}_c| + |\mathbf{x}_X-\mathbf{x}_s|\right\}\right], \quad (21)$$

$$\Omega_3 = \omega\left[t - c_0^{-1}\left\{|\mathbf{x}_B-\mathbf{x}_c| + 2|\mathbf{x}_c-\mathbf{x}_s| - |\mathbf{x}_X-\mathbf{x}_s| - |\mathbf{x}_A-\mathbf{x}_s| + |\mathbf{x}_X-\mathbf{x}_c|\right\}\right], \quad (22)$$

$$\Omega_4 = \omega\left[t - c_0^{-1}\left\{|\mathbf{x}_B-\mathbf{x}_c| - |\mathbf{x}_A-\mathbf{x}_c|\right\}\right]. \quad (23)$$

We analyze these rapid phases using the stationary-phase method, keeping $\mathbf{x}_A$ and $\mathbf{x}_B$ fixed and varying $\mathbf{x}_X$, $\mathbf{x}_c$ and $\mathbf{x}_s$. According to the stationary-phase method, the dominant contribution to the integral and sum in equation 19 comes from positions of $\mathbf{x}_X$, $\mathbf{x}_c$ and $\mathbf{x}_s$ where

$$\partial_\omega\Omega = 0, \qquad \nabla_{\mathbf{x}_s}\Omega = \mathbf{0}, \qquad \nabla_{\mathbf{x}_X}\Omega = \mathbf{0} \quad \text{and} \quad \nabla_{\mathbf{x}_c}\Omega = \mathbf{0} \quad (24)$$

From the rapid phase, Ω_1, of the first term in equation 19 we find stationary points for which

$$t = c_0^{-1}\left\{|\mathbf{x}_B-\mathbf{x}_s| - |\mathbf{x}_A-\mathbf{x}_s|\right\}, \quad (25)$$

$$\nabla_{\mathbf{x}_s}|\mathbf{x}_B-\mathbf{x}_s| = \nabla_{\mathbf{x}_s}|\mathbf{x}_A-\mathbf{x}_s|, \quad (26)$$

$$\nabla_{\mathbf{x}_X}|\mathbf{x}_B-\mathbf{x}_s| = \nabla_{\mathbf{x}_X}|\mathbf{x}_A-\mathbf{x}_s|, \quad (27)$$

$$\nabla_{\mathbf{x}_c}|\mathbf{x}_B-\mathbf{x}_s| = \nabla_{\mathbf{x}_c}|\mathbf{x}_A-\mathbf{x}_s|. \quad (28)$$

Conditions 27 and 28 are always satisfied. Condition 26 requires the stations to be on a line and the source to be on a line issuing from $\mathbf{x_s}$. When the stations and source are aligned as $\mathbf{x}_s \to \mathbf{x}_A \to \mathbf{x}_B$, condition 25 gives $t = c_0^{-1}|\mathbf{x}_B-\mathbf{x}_A|$. When the stations and source are aligned as $\mathbf{x}_s \to \mathbf{x}_B \to \mathbf{x}_A$, the first condition gives $t = -c_0^{-1}|\mathbf{x}_B-\mathbf{x}_A|$.

From the rapid phase, Ω_2, of the first term in equation 19 we find stationary points for which

$$t = c_0^{-1}\left\{|\mathbf{x}_B-\mathbf{x}_s| - |\mathbf{x}_X-\mathbf{x}_c| - 2|\mathbf{x}_c-\mathbf{x}_s| - |\mathbf{x}_A-\mathbf{x}_c| + |\mathbf{x}_X-\mathbf{x}_s|\right\}, \quad (29)$$

$$\nabla_{\mathbf{x}_s}\left\{|\mathbf{x}_B-\mathbf{x}_s| - |\mathbf{x}_c-\mathbf{x}_s|\right\} = \nabla_{\mathbf{x}_s}\left\{|\mathbf{x}_c-\mathbf{x}_s| - |\mathbf{x}_X-\mathbf{x}_s|\right\}, \quad (30)$$

$$\nabla_{\mathbf{x}_X}|\mathbf{x}_X-\mathbf{x}_c| = \nabla_{\mathbf{x}_X}|\mathbf{x}_X-\mathbf{x}_s|, \quad (31)$$

$$-\nabla_{\mathbf{x}_c}\left\{|\mathbf{x}_c-\mathbf{x}_s| + |\mathbf{x}_X-\mathbf{x}_c|\right\} = \nabla_{\mathbf{x}_c}\left\{|\mathbf{x}_A-\mathbf{x}_c| + |\mathbf{x}_c-\mathbf{x}_s|\right\}. \quad (32)$$

Condition 30 requires that station B, auxiliary station, the scatterer are on a line issuing from the source. Condition 31 requires that the auxiliary station and the scatterer are on a line issuing from the source. Condition 32 requires that station A, an auxiliary station and a scatterer are on a line issuing from the source. In short, stations A and B, an auxiliary station, and the scatterer all align on a line issuing from the source. When these are aligned as $\mathbf{x_s} \rightarrow \mathbf{x}_c \rightarrow \mathbf{x}_X \rightarrow \mathbf{x}_A \rightarrow \mathbf{x}_B$, then $|\mathbf{x}_X - \mathbf{x}_s| = |\mathbf{x}_X - \mathbf{x}_c| + |\mathbf{x}_c - \mathbf{x}_s|$, $|\mathbf{x}_c - \mathbf{x}_s| + |\mathbf{x}_A - \mathbf{x}_c| = |\mathbf{x}_A - \mathbf{x}_s|$, and condition 29 gives $t = c_0^{-1}|\mathbf{x}_B - \mathbf{x}_A|$. When stations A and B are reversed, condition 29 gives $t = -c_0^{-1}|\mathbf{x}_B - \mathbf{x}_A|$.

The rapid phase, Ω_3, of the third term in equation 19 is similar to the rapid phase, Ω_2, of the second term in equation 19. If stations A, B, an auxiliary station, and the scatterer are located on a line issuing from the source, aligned as $\mathbf{x_s} \rightarrow \mathbf{x}_c \rightarrow \mathbf{x}_X \rightarrow \mathbf{x}_A \rightarrow \mathbf{x}_B$, the dominant contribution resides at $t = c_0^{-1}|\mathbf{x}_B - \mathbf{x}_A|$. When stations A and B are interchanged, the dominant contribution of the third term in equation 19 resides at $t = -c_0^{-1}|\mathbf{x}_B - \mathbf{x}_A|$. Last we analyze the rapid phase, Ω_4, of the fourth term in equation 19, and we find stationary points for which

$$t = c_0^{-1}\left\{|\mathbf{x}_B - \mathbf{x}_c| - |\mathbf{x}_A - \mathbf{x}_c|\right\}, \tag{33}$$

$$\nabla_{\mathbf{x}_s}|\mathbf{x}_B - \mathbf{x}_c| = \nabla_{\mathbf{x}_s}|\mathbf{x}_A - \mathbf{x}_c|, \tag{34}$$

$$\nabla_{\mathbf{x}_X}|\mathbf{x}_B - \mathbf{x}_c| = \nabla_{\mathbf{x}_X}|\mathbf{x}_A - \mathbf{x}_c|, \tag{35}$$

$$\nabla_{\mathbf{x}_c}|\mathbf{x}_B - \mathbf{x}_c| = \nabla_{\mathbf{x}_c}|\mathbf{x}_A - \mathbf{x}_c|. \tag{36}$$

Conditions 34 and 35 are always satisfied. Condition 36 is satisfied when the scatterer lies on a line through stations A and B. When stations A, B and the scatterer are aligned as $\mathbf{x}_c \rightarrow \mathbf{x}_A \rightarrow \mathbf{x}_B$, condition 33 gives $t = c_0^{-1}|\mathbf{x}_B - \mathbf{x}_A|$. When stations A, B and the scatterer align as $\mathbf{x}_c \rightarrow \mathbf{x}_B \rightarrow \mathbf{x}_A$, condition 33 gives $t = -c_0^{-1}|\mathbf{x}_B - \mathbf{x}_A|$.

EXAMPLE OF GREEN'S FUNCTION ITERATED CORRELATION

We next study how forming $C^{(3)}_{B,A}$ of a wave field excited by a single source can improve the retrieved Green's function in the presence of an auxiliary scatterer. We study a geometry where the main stations are located 200 m distant from each other (see Figure 6). We use 512 auxiliary stations located on a circle with radius 300 m centered between the two main stations. The source is located at s', with a distance of 800 m from the center and at an angle of $\phi = 3/4\pi$ radians. There is a scatterer positioned at a distance of 550 m from the center at an angle of $\phi = \pi$ radians. We omit the terms of group 3 in equation 15, because their contribution is at least of order α weaker than those in group 2. $C^{(2)}$ is evaluated between stations A or B and all the auxiliary stations X, yielding $C^{(2)}_{A,X}$ and $C^{(2)}_{B,X}$; the obtained correlograms are shown in Figures 7(a) and 7(b). We evaluate $C^{(3)}_{B,A}$ for each auxiliary station, including all terms of groups 1 and 2, and compile the result in a correlogram shown in Figure 8(a).

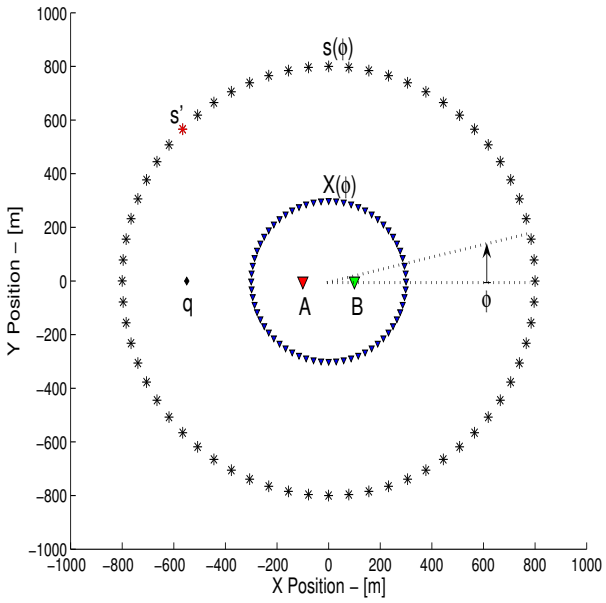

Figure 6: Experiment geometry for the evaluation of $C^{(3)}_{B,A}$. [**ER**]

The contribution of each term is labeled according to the numbering of equation 15. We sum $C^{(3)}_{B,A}$ over the auxiliary stations, according to equation 18, to obtain the retrieved signal in Figure 8(b). We compare this signal to the true result, convolved with the square of the autocorrelation of the wavelet $S(\omega)$, and the result retrieved by correlating stations B and A directly ($C^{(2)}_{B,A}$) weighted by $-i\omega S(\omega)$. It is clear that the dominant contribution in $C^{(3)}_{B,A}$, without muting $C^{(2)}_{A,X}$ and $C^{(2)}_{B,X}$, does not correspond to the direct event between the stations A and B. If we assume we can perfectly mute only the dominant term 4.1 from $C^{(2)}_{A,X}$ and $C^{(2)}_{B,X}$, this would leave the terms of group 2.

A correlogram of their contributions to $C^{(3)}_{B,A}$ is shown in Figure 9(a), summing this panel and multiplying with a phase-modifying according to equation 18, leads to the signal in Figure 9(b). We now see that there is a dominant term coinciding with the causal direct event between stations A and B in the true result; this event comes from term 15.11.

ITERATED CORRELATION AFTER MUTING

The terms in group 2 cannot uniquely be separated from those of groups 1. Time-domain muting of $C^{(2)}_{B,X}$ and $C^{(2)}_{B,X}$ can exclude the leading order event 4.1, but would also exclude parts of terms 4.2 and 4.3. The black lines in Figures 7(a) and 7(b) indicate the travel time of an event between station A or B and each auxiliary station. The dominant term in $C^{(2)}$ will always reside in this window, see Figure 4(a). We now mute each $C^{(2)}$ according to these limits to obtain the two correlograms in Figures 10(a) and 10(b).

The $C^{(3)}_{B,A}$ is evaluated for each auxiliary station to obtain the correlogram in

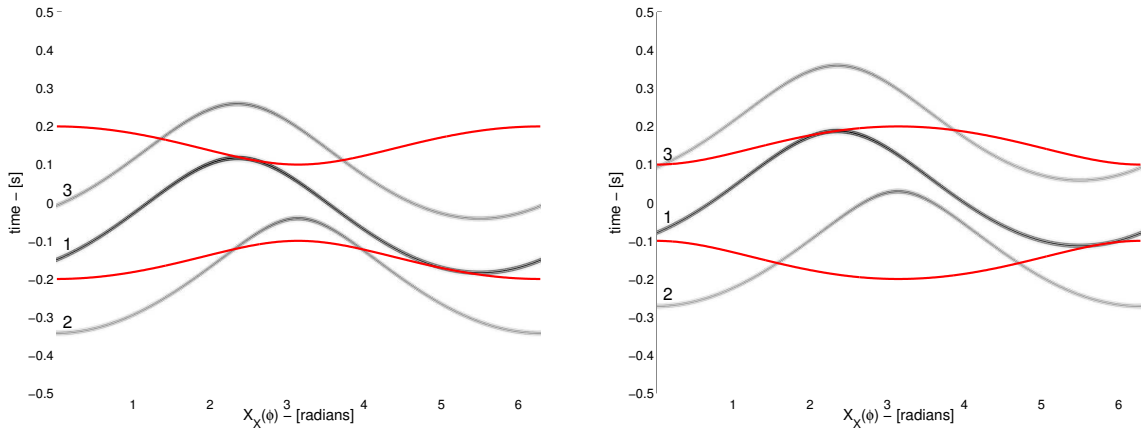

(a) (b)

Figure 7: a) Correlogram for correlations between station A and all auxiliary stations as a function of auxiliary station-position angle. Black lines indicates traveltime of a wave from station A to each auxiliary station. b) Correlogram for correlations between station B and all auxiliary stations as a function of auxiliary station-position angle. Black line indicates traveltime of a wave from station or B to each auxiliary station. [**ER**]

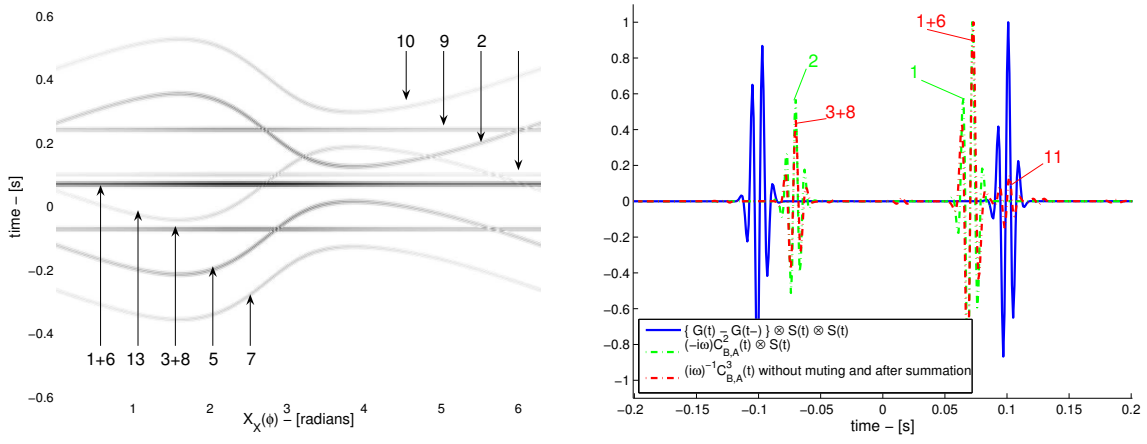

(a) (b)

Figure 8: a) Correlogram of $C^{(3)}_{B,A}$ for each auxiliary station, including all 11 terms in groups 1 and 2 of equation 15. b) Correlogram of $C^{(3)}_{B,A}$ for each auxiliary station, including only the 4 terms from groups 2 of equation 15. [**ER**]

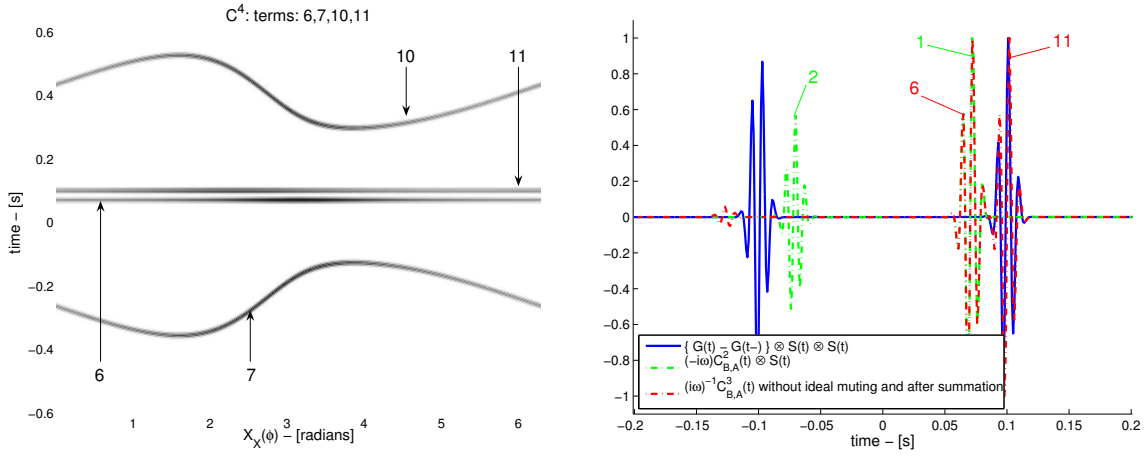

(a) (b)

Figure 9: a) Comparison of reconstructed Green's function with the true result, after summation of all 11 terms of groups 1 and 2 over auxiliary station. b) Comparison of reconstructed Green's function with true result, after summation of 4 terms of group 2 over auxiliary station. [**ER**]

Figure 11(a), this panel is summed and multiplied with a phase-modifying according to equation 18 to retrieve the signal in Figure 11(b).

The resulting signal resembles the true result slightly better than evaluating the terms of equation 15 group 2 without muting; the spurious event arriving at $t = .8$s is slightly smaller. This is because, for the present geometry, the auxiliary stations where the spurious event is absent, would have contributed more strongly to the spurious event without muting before evaluating $C^{(3)}_{B,A}$. (The geometrical spreading factors vary for the contribution of each auxiliary station.)

ITERATED CORRELATION DEPENDANCE ON SOURCE POSITION

For the geometry in Figure 6, the source, stations A and B, auxiliary stations and scatterer are not aligned at a stationary phase of terms 15.6, 15.7 and 15.10. We will investigate the retrieved result of evaluating $C^{(3)}_{B,A}$ after muting $C^{(2)}_{A,X}$ and $C^{(2)}_{B,X}$, and summing over all auxiliary stations and multiplying with the phase-modifying factor as in equation 18. The sources are positioned on a circle with radius 800 m centered between stations A and B in the geometry described as before; see Figure 6. Evaluating $C^{(3)}_{B,A}$ and summation over the auxiliary stations for terms 15.6 15.7, 15.10 and 15.11, and then evaluating equation 18 for each source contribution gives the correlogram in Figure 12(a).

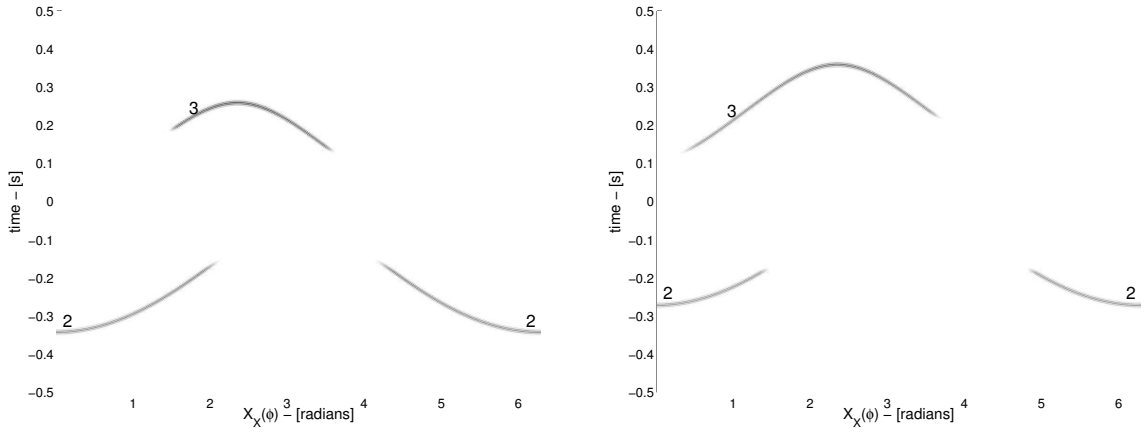

(a) (b)

Figure 10: Muted $C^{(2)}_{A,X}$ in a) and $C^{(2)}_{B,X}$ in b). These are the input for the evaluation of $C^{(3)}_{B,A}$. [**ER**]

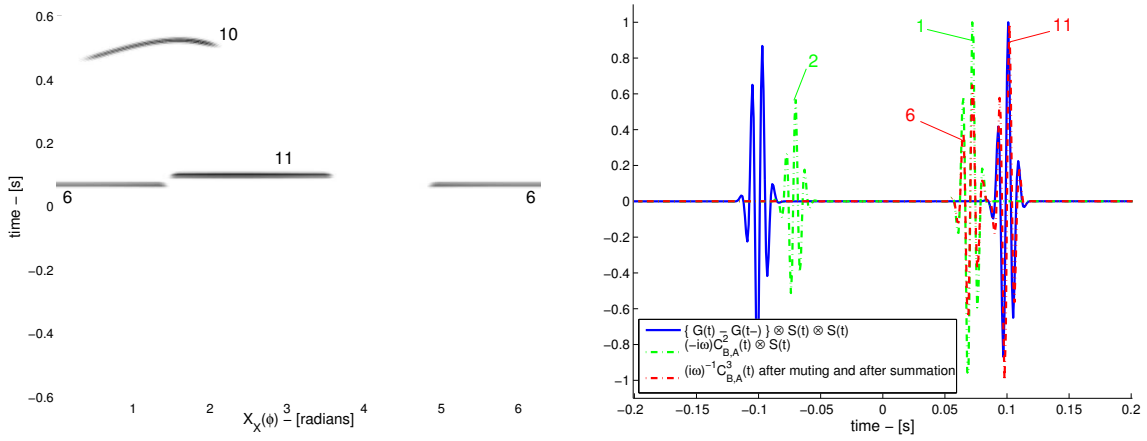

(a) (b)

Figure 11: a) Correlogram of $C^{(3)}_{B,A}$ evaluated after muting $C^{(2)}$, as a function of each auxiliary station-position angle ϕ. b) Comparison of retrieved Green's function with the true result, after summation of $C^{(3)}_{B,A}$ over all auxiliary stations. [**ER**]

This correlogram confirms that when the source, stations A and B, an auxiliary station, and the scatterer are aligned, each term has a stationary phase. We also see how term 15.11 is stationary with respect to source postion. The behavior of term 15.6 is similar to that of the leading term in $C^{(2)}_{B,A}$; see Figure 4(a). This can be expected from the constraint on t in condition 25, which is equal to condition 11 on t for $C^{(2)}_{B,A}$. We can expect that when we time-average the $C^{(3)}_{B,A}$ of multiple sources at different angular positions, term 15.6 interferes destructively.

Figure 12(a) also tells us that terms 15.7 and 15.10 are also non-stationary with respect to source position. However, the arrival time of non-stationary positions is dependent upon scatterer position (see condition 29); this implies that in a medium with randomly positioned scatterers, terms 15.7 and 15.10 would interfere destructively. Last we investigate whether muting $C^{(2)}$ before evaluating $C^{(3)}_{B,A}$ can work for the source postions located at stationary phases for terms 15.6 15.7 and 15.10; see Figure 12(b). We see how muting the $C^{(2)}_{A,X}$ and $C^{(2)}_{B,X}$ for source positions at and close to $\phi = \pi$ radians also would remove the energy associated with the scatterer. This is expected, because the scatterer is directly behind the source as seen from both stations A and B; thus the contribution arrives simultaneously with the direct event from the source.

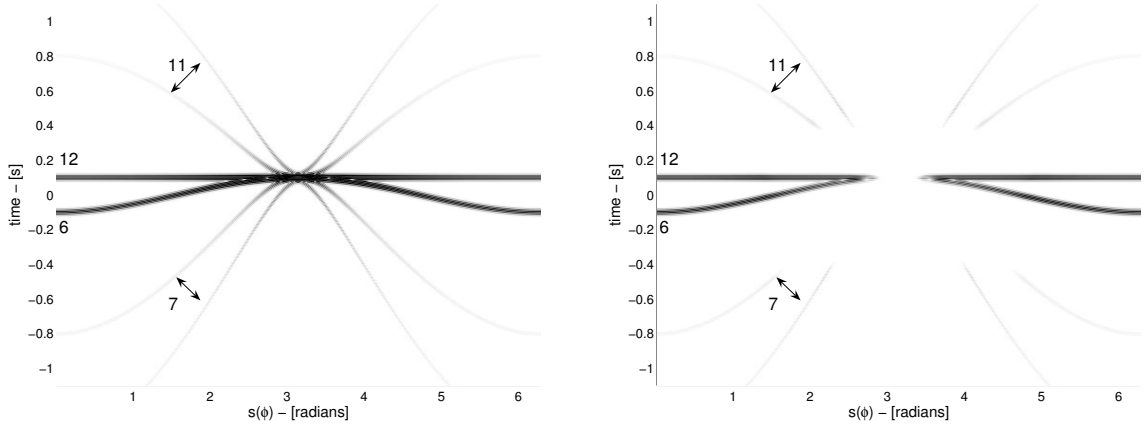

(a) (b)

Figure 12: a) Gather showing time-domain equivalents of 15.6, 15.7, 15.10 and 15.11 after summing over auxiliary stations as a function of source position angle ϕ. b) Gather of $|\tilde{C}^{3}_{B,A}(t)|$ as a function of source position angle ϕ. [**ER**]

CONCLUSIONS

Using Green's functions under the Born approximation in a homogeneous medium with one scatterer, we show that $C^{(3)}_{B,A}$ constitutes 16 terms, that can be divided into 3 groups. The leading-order terms, group 1, are associated with the correlation

of the direct waves recorded at the stations from a source that is generally not at a stationary-phase position. Thus evaluating $C^{(3)}_{B,A}$ directly does not improve the Green's function estimation. Instead we can remove the terms in group 1 from $C^{(3)}_{B,A}$ by muting $C^{(2)}_{A,X}$ and $C^{(2)}_{B,X}$. Group 2 contains the 4 leading-order terms in $C^{(3)}_{B,A}$ after muting $C^{(2)}_{B,X}$ and $C^{(2)}_{B,X}$. A stationary-phase ananysis of the 4 terms tells us that the scatterer must be aligned on ray paths between two stations, outside the station span.

Term 15.6 is non-stationary for all source postitions not aligned with the scatterer and stations A and B. The non-stationarity is a function only of source position, not of auxiliary-station position. When we evaluate an ensemble average of multiple sources from different locations, term 15.6 will, in general, interfere destructively. Terms 15.7 and 15.10 are stationary when the source aligns with the scatterer, an auxiliary station and stations A and B. The non-stationarity is a function of source position and of auxiliary-station position. We can exploit this fact by using a network of auxiliary stations positioned randomly, such that if the source position is not at the stationary phase, the contribution from different auxiliary stations stack incoherently. Only term 15.11 remains stationary no matter where the source or auxiliary stations are positioned, so that any stacking of $C^{(3)}_{B,A}$ over auxiliary stations will enhance the contribution of this term.

An additional problem for the utilization of terms 15.6, 15.7 and 15.10 for the improvement of Green's function reconstruction is that for the source position for which these terms have stationary contributions at the correct traveltime, the contribution becomes indistinguishable from the leading-order contribution in $C^{(2)}_{A,X}$ and $C^{(2)}_{B,X}$ that must be removed. This means that stacking is the key to enhancing the contribution of term 15.11 and diminishing the contributions of terms 15.6, 15.7 and 15.10 to the EGF from $C^{(3)}_{B,A}$.

APPENDIX

WAVE EQUATION AND GREEN'S FUNCTION

We study the wave equation in an acoustic, linear, isotropic, time-invariant, sourceless, constant-density medium. The familiar wave equation for pressure $P = P(\mathbf{x}, t)$ is

$$\partial_i^2 P - c^{-2}\partial_t^2 P = 0, \tag{A-1}$$

where Einstein's summation convention is applied to lower-case subscripts; for 2D they are summed over 1 and 2. Temporal and spatial derivatives are denoted ∂_t and ∂_i respectively, where the subscripts denote time and spatial directions respectively. Under the constant-density assumption, the characteristic wave velocity $c = c(\mathbf{x})$ fully determines the medium.

Fourier Transformations

The temporal Fourier transformation pairs of a time-domain function $F(t)$ and frequency-domain function $F(\omega)$ are defined as

$$F(\omega) = \int_{\infty}^{-\infty} F(t)\, \exp\left(-i\omega t\right) \mathrm{d}t, \tag{A-2}$$

$$F(t) = \frac{1}{2\pi} \int_{\infty}^{-\infty} F(\omega)\, \exp\left(i\omega t\right) \mathrm{d}\omega, \tag{A-3}$$

the particular Fourier-domain of the function F is specified by the argument only.

Frequency-domain Green's function in homogeneous media

Using the forward Fourier transformation equation A-2, the wave equation for pressure in a homogeneous medium with $c(\mathbf{x}) = c_0$ is written in the frequency-domain as

$$\partial_i^2 P + \frac{\omega^2}{c_0^2} P = 0. \tag{A-4}$$

The frequency-domain Green's function $G = G(\mathbf{x}, \mathbf{x}_s, \omega)$ is defined by introducing an impulsive point source acting at $t = 0$ and $\mathbf{x} = \mathbf{x}_s$ on the right-hand side of equation A-4 as follows:

$$\partial_i^2 G + \frac{\omega^2}{c_0^2} G = -\delta(\mathbf{x} - \mathbf{x}_s). \tag{A-5}$$

The Green's function solution for two-dimensional space, under the far field approximation can be obtained as

$$G(\mathbf{x}, \mathbf{x}_s, \omega) = \frac{1}{\sqrt{8\pi\omega c_0^{-1} \left|\mathbf{x} - \mathbf{x}_s\right|}} \exp\left(-i\left[\omega c_0^{-1} \left|\mathbf{x} - \mathbf{x}_s\right| + \frac{\pi}{4}\right]\right). \tag{A-6}$$

A source function is easily included by multiplication with the frequency-domain source function. A measurement, $P_A(\omega)$, at a station located at $\mathbf{x}_A$ of a source at $\mathbf{x}_s$ emitting a source function $s(\omega)$ is obtained as follows:

$$P_A = G(\mathbf{x}_A, \mathbf{x}_s, \omega) s(\omega). \tag{A-7}$$

The sources in this paper are simulated emitting zero-phase Ricker wavelets with center frequency ω_0. The frequency-domain expression used is

$$s(\omega) = \frac{2\,\omega^2}{\sqrt{\pi}\,\omega_0^3} \exp\left(-\frac{\omega^2}{\omega_0^2}\right). \tag{A-8}$$

Green's function in the Born Approximation

We are interested in the Green's function in an inhomogeneous medium. We assume the velocity can be split into a background velocity c_0 and a perturbation $\alpha(\mathbf{x})$ as $c^{-2}(\mathbf{x}) = c_0^{-2}\left[1+\alpha(\mathbf{x})\right]$. Assuming the perturbation is confined inside some finite domain $\mathbf{D}_s$, the Green's function in the Born approximation can now be computed in terms of a Green's function computed in the background, G_0, medium as

$$G(\mathbf{x},\mathbf{x}_s,\omega) = G_0(\mathbf{x},\mathbf{x}_s,\omega) + G_1(\mathbf{x},\mathbf{x}_s,\omega), \quad \text{with} \tag{A-9}$$

$$G_1(\mathbf{x},\mathbf{x}_s,\omega) = \oint_{\mathbf{D}_s} G_0(\mathbf{x},\mathbf{x}',\omega)\frac{\omega^2}{c_0^2}\alpha(\mathbf{x}')G_0(\mathbf{x}',\mathbf{x}_s,\omega)\mathrm{d}\mathbf{x}'. \tag{A-10}$$

The Green's function in the background medium is computed using equation A-5 with $c = c_0$. When the medium consists of a homogeneous background with a series of N scatters positioned at $\mathbf{x}_{c,1},\mathbf{x}_{c,2},\mathbf{x}_{c,3}...\mathbf{x}_{c,N}$ with strength $\alpha_1,\alpha_2,\alpha_3,...\alpha_N$, then $\alpha(\mathbf{x}) = \sum_{i=1}^{N}\delta(\mathbf{x}-\mathbf{x}_{c,i})\alpha_i$. Hence the Green's function G_1 in equation A-10 can be written as

$$G_1(\mathbf{x},\mathbf{x}_s,\omega) = \sum_{i=1}^{N} G_0(\mathbf{x},\mathbf{x}_{c,i},\omega)\frac{\omega^2}{c_0^2}\alpha_i G_0(\mathbf{x}_{c,i},\mathbf{x}_s,\omega). \tag{A-11}$$

REFERENCES

Aki, K., 1957, Space and time spectra of stationary stochastic waves, with special reference to microtremors: Bulletin of the Earthquake Research Institute, **35**, 415–456.

Claerbout, J. F., 1968, Synthesis of a layered medium from its acoustic transmission response: Geophysics, **33**, 264–269.

———, 1976, Fundamentals of Geophysical Data Processing; with Applications to Petroleum Prospecting: Blackwell Scientific Publications.

de Ridder, S., 2008, Seismic interferometry versus spatial auto-correlation method on the regional coda of the NPE: Technical report, SEP-136.

Garnier, J. and G. Papanicolaou, 2009, Passive sensor imaging using cross correlations of noisy signals in a scattering medium: SIAM J. Imaging Sci., **2**, 396–437.

Lobkis, O. I. and R. L. Weaver, 2001, On the emergence of the greens function in the correlations of a diffuse field: J. Acoust. Soc. Am., **110**, 3011–3017.

Malcolm, A. E., J. A. Scales, and B. A. van Tiggelen, 2004, Retrieving the green function from diffuse, equipartitioned waves: Phys. Rev. E., **70**, 015601–1–015601–4.

Paul, A., M. Campillo, L. Margerin, E. Larose, and A. Derode, 2005, Empirical synthesis of time-asymmetrical Green functions from the correlation of coda waves: Journal of Geophysical Research (Solid Earth), **110**, B08302.1–B08302.13.

Roux, P., K. G. Sabra, W. A. Kuperman, and A. Roux, 2005, Ambient noise cross correlation in free space: Theoretical approach: JASA, **117**, 79–84.

Ruigrok, E. N., D. S. Dragonov, J. Thorbecke, J. R. van der Neut, and K. Wapenaar, 2008, Sampling and illumination aspects of seismic interferometry in horizontally layered media: 70th EAGE annual meeting, Rome, Italy., P277.

Sánchez-Sesma, F. J. and M. Campillo, 2006, Retrieval of the Green's function from cross correlation: The canonical elastic problem: Bull. Seism. Soc. Am., **96**, 1182–1191.

Sánchez-Sesma, F. J., J. A. Párez-Ruiz, M. Campillo, and F. Luzón, 2006, Elastodynamic 2D Green's function retrieval from cross-correlation: Canonical inclusion problem: Geophys. Res. Let., **33**, L13305–1–L13305–6.

Schuster, G. T., J. Yu, J. Sheng, and J. Rickett, 2004, Interferometric/daylight seismic imaging: Geophys. J. Int., **157**, 838–852.

Snieder, R., K. van Wijk, M. Haney, and R. Calvert, 2008, The cancellation of spurious arrivals in Green's function extraction and the generalized optical theorem: Phys. Rev. E, **78**, 036606–1–036606–8.

Snieder, R., K. Wapenaar, and K. Larner, 2006, Spurious multiples in seismic interferometry of primaries: Geophysics, **71**, SI111–SI124.

Snieder, R., K. Wapenaar, and U. Wegler, 2007, Unified Green's function retrieval by cross-correlation; Connection with energy principles: Phys. Rev. E, **75**, 036103–1–036103–14.

Snieder, R. K., 2004, Extracting the Green's function from the correlation of coda waves: A derivation based on stationary phase: Phys. Rev. E, **69**, 046610–1–046620–8.

Stehly, L., M. Campillo, B. Froment, and R. L. Weaver, 2008, Reconstructing Green's function by correlation of the coda of the correlation (C^3) of ambient seismic noise: J. Geophys. Res., **113**, B11306.1–B11306.10.

Stork, C. and S. Cole, 2007, Fixing the nonuniform directionality of seismic daylight interferometry may be crucial to its success: SEG Technical Program Expanded Abstracts, **26**, 2713–2717.

van der Neut, J. and A. Bakulin, 2008, The effects of time?gating and radiation correction on virtual source data: SEG, Expanded Abstracts, **27**, 2922–2926.

van der Neut, J. R., A. Bakulin, and K. Mehta, 2008, The effects of time-gating and radiation correction on virtual source data: 70th EAGE annual meeting, Rome, Italy., P274.

van Manen, D.-J., J. O. A. Robertsson, and A. Curtis, 2005, Modeling of wave propagation in inhomogeneous media: Phys. Rev. Lett., **94**, 164301–1–164301–4.

Wapenaar, K., 2004, Retrieving the elastodynamic Green's function of an arbitrary inhomogeneous medium by cross correlation: Phys. Rev. Lett., **93**, 254301–1 – 254301–4.

Wapenaar, K. and J. Fokkema, 2006, Green's function representations for seismic interferometry: Geophysics, **71**, SI33–SI46.

Wapenaar, K., J. van der Neut, and E. Ruigrok, 2008, Passive seismic interferometry by multidimensional deconvolution: Geophysics, **73**, A51–A56.

Weaver, R. L. and O. I. Lobkis, 2001, Ultrasonics without a source: Thermal fluctuation correlations at mhz frequencies.: Phys. Rev. Let., **87**, 134301.1–134301.4.

———, 2004, Diffuse fields in open systems and the emergence of the Green's function

(L): J. Acoust. Soc. Am., **116**, 2731–2734.